Journal of Magnetism and Magnetic Materials 458 (2018) 10–14

Contents lists available at ScienceDirect

Journal of Magnetism and Magnetic Materials

journal homepage: www.elsevier.com/locate/jmmm

Research articles

Multiferroic property of $Ca_{1-x}La_xTi_{1-x}Fe_xO_3$ perovskite structure

L.M. Salah [a], A.F. Mabied [b,c], M.H. Abdellatif [b,*]

[a] Physics Department, Faculty of Science, Cairo University, Egypt
[b] Solid State Physics Department, National Research Centre, Dokki, Cairo, Egypt
[c] Department of Basic Science, October High Institute of Engineering & Technology – OHI, 2nd Neighbourhood, 3rd District, 6th of October, Giza, Egypt

ARTICLE INFO

Article history:
Received 1 December 2017
Received in revised form 24 January 2018
Accepted 19 February 2018
Available online 20 February 2018

Keywords:
Multiferroic
Perovskite
Crystal symmetry

ABSTRACT

We studied the multiferroic property of $Ca_{1-x}La_xTi_{1-x}Fe_xO_3$ ($0.0 \leq x \leq 0.5$) perovskite. We showed that multiferroic property can be triggered by strain mediation due to different ion doping. The prepared samples were characterized by X-ray to check for its phase purity. Increasing the La^{3+} ion concentration is found to induce a crystal distortion. A pseudo-tetragonal phase is found at the highest La^{3+} ion concentration. The changes in crystal symmetry induce different effects on the electrical polarization that can be seen in the electrical hysteresis of the perovskite. The correlation between magnetic and electric ordering reduces as the concentration of La^{3+} ion increases in which the lattice symmetry are more close to space invariant. The changes in the vibrational bands due to changes in the crystal structure were investigated by FTIR.

1. Introduction

The coupling between magnetic and electrical ordering is known as multiferroicity [1,2]. Multiferroic materials are rare in nature since ferroelectric and ferromagnetic requirements are quite different. The ferro-electricity arises due to empty d-shells while ferromagnetism requires partially filled d-shells. It turns out having both criteria in the same material are not feasible. Several trials were done so far to fabricate multiferroic materials, by mixing of two solid solutions of ferroelectric and ferromagnetic, or by doping the ferroelectric material with magnetic ions [3–5]. Special symmetry condition is required in order for both ferroic properties to be present at the same phase in the crystal [6,7]. In general breaking symmetry could be the reason for many fascinating physical properties [8]. The discovery of large ferroelectric polarization for epitaxial bithmus ferrite were first reported in Ref. [9] in which the existence of non-collinear magnetic ordering is considered a reason for multiferroic by triggering the ferroelectricity [10,11]. However, the main aspect of the multiferroic is that the magnetic ordering and electric ordering exclude each other. In general, the polarization P of the charge dipoles can be reversed under space inversion which does not affect the magnetization M, while the time invariance affects the sign of M and does not change the dipole symmetry. Hence we can say that the ferroelectrics are invariant under time reversal and ferromagnetic are invariant under space reversal, the statement cannot be reversed. Hence, it is obvious that multiferroic violates the previous statement since they are both time and space invariant at the same phase, where the mutual exclusion of properties are not valid.

However, there are two categories for multiferroic materials A, and B [12]. Class A, is highly ordered ferroelectric with antiferromagnetic properties, that exhibit lower magnetic ordering temperature, such as $BiFeO_3$, $YMnO_3$. In Class B, the magnetic ordering induces ferroelectricity, the magnetic and electric ordering temperature are identical and low, all rare earth manganites such as $HoMn_2O_5$, $TbMnO_3$ fall in that category [12]. Those categories are known as single-phase multiferroic, while composites of two ferroic phase can show similar multiferroic properties in which each phase behaves independently. The first multiferroic composite was introduced in the 1960s by combining two ferroic phases [13]. However, combining the ferro-electricity and ferromagnetic properties in one system depends on the coupling strength and the symmetry of crystal lattice [14–19]. However, the microscopic view of the magnetic ordering relies on the exchange interaction of the localized magnetic moments, if the material consists of separate units, then it is possible to formulate a composite that induces both ferromagnetic and ferroelectric properties. A noncentrosymmetric structure that contains magnetic ions is then expected to exhibit both properties of ferromagnetic and ferroelectricity in the same phase, but the coupling between the magnetic and electric properties may not be strong [20]. The mutual exclusion of the magnetic and electric properties in perovskite is still valid, although it is considered a promising structure for multifer-

* Corresponding author at: National Research Center, 12622 Giza, Egypt.
E-mail address: cds.moh@gmail.com (M.H. Abdellatif).

https://doi.org/10.1016/j.jmmm.2018.02.062
0304-8853/

roic applications [21]. The emptiness of the d-shell in the transition metal perovskite is a common property, although not sufficient but necessary condition for ferroelectric property to exist, but it will roll out the magnetic ordering. Hence there should be a different way to initiate the ferro-electricity while keeping the d-shell half filled. The geometrical distortion could be the solution, where the doping metal is shifted off-center in the octahedra. The off-center shift allows a stronger metal-oxygen bond on one side and weaker on another side [7,18]. The spatial difference in the oxygen- metal covalent bond strength is sufficient to induce ferroelectricity. However, it requires an empty d-shell for the ion to establish the covalent bond, which means ferromagnetism, is expected in case of non-empty d-shell in a centrosymmetric lattice. The ferroelectricity can be expected in the same lattice configuration if the electron hybridization can cause the metal d-shell appears temporarily empty. Hence doping could be the technique to have covalent bonding of different strength, which in turn triggers the multiferroic property [19,22].

In this work, we show that a system of multiple element doping in perovskite structure of the general formula $Ca_{1-x}La_xTi_{1-x}Fe_xO_3$ shows magnetic and electric properties simultaneously in the same phase, which could be due to temporary empty d-shell due to the strong hybridization that initiates the ferroelectricity in the ferromagnetic structure.

2. Experimental procedure

The perovskite structure with the chemical formula $Ca_{1-x}La_xTi_{1-x}Fe_xO_3$, $0.0 \leqslant x \leqslant 0.5$ were prepared by solid-state reaction at 1350 °C for 24 h. The detailed procedure of preparation process can be found in a previous publication [16,23,24]. The FTIR results were performed using spectrometer (Jasco 6300, Japan) at room temperature in the range 4000–400 cm^{-1} and 650–150 cm^{-1}. The magnetic hysteresis was carried out using vibrating sample magnetometer (9600-1 LDJ, USA), at temperature 70 K, 100 K, 150 K, 200 K, 250 K. The Dc conductivity was measured using a homemade circuit, and the electrical hysteresis was performed using a modified Sawyer-Tower bridge [25]. An oscilloscope (GDS-2204 digital type) was used to characterize the

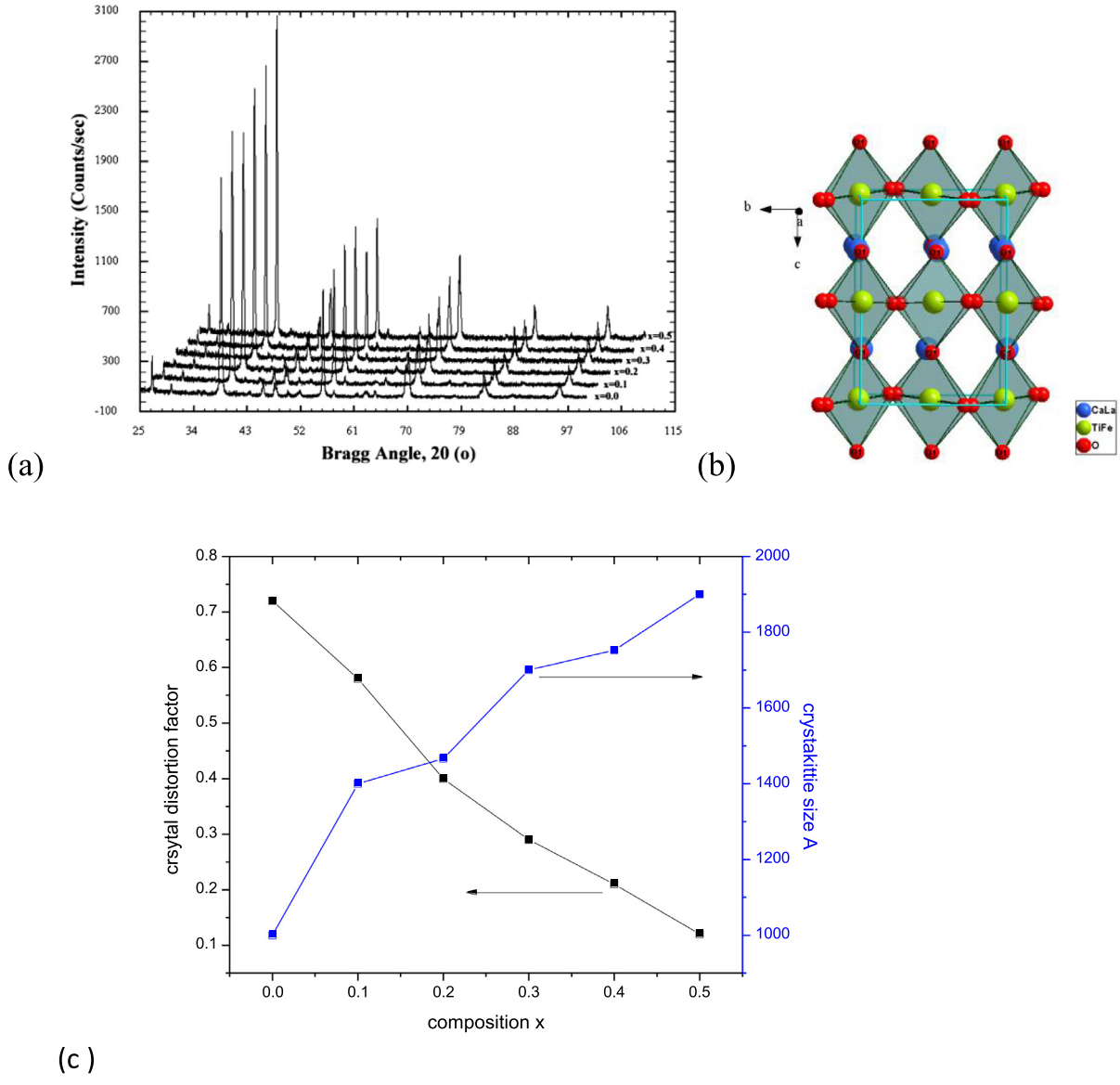

Fig. 1. (a–c): XRD for the perovskite structure of different La^{3+} ion doping concentration, (b) Crystal structure of the perovskite structure as predicted from structure simulation software. (c) Variation of the crystal distortion factor and the crystal size with the composition x, the data are based on the Rietveld analysis.

polarizing voltage. A linear capacitor C_o is connected in series with the sample, the voltage across C_o is therefore proportional to the polarization of the sample. The technique allows measurement of important quantities such as the spontaneous polarization P_s and the coercive field E_c. More details about the technique can be found in the references [25,26].

3. Results

Fig. 1a shows the X-ray diffraction micrographs for five samples of perovskite structure $Ca_{1-x}La_xTi_{1-x}Fe_xO_3$, $0.0 \leqslant x \leqslant 0.5$, the peak indexing was done by comparing the samples with JCPDS card number (81-0562). The disappearance of oxides diffraction peaks confirms the orthorhombic single phase of the prepared samples. A detailed description of the Rietveld refinement for the samples could be found in Ref. [24]. The Rietveld refinement shows a non-centrosymmetric structure of space group Pbnm for all the prepared samples. The maximum distortion is found for $CaTiO_3$, where the cell distortion is found to decrease as the substituted metal ion concentration increase, at x = 0.5 the cell reaches a pseudo-tetragonal structure. Fig. 1b shows a schematic diagram of the structure, while the variation of the crystallite size and cell distortion factor with changing the ion concentration x is shown in Fig. 1c. It can be seen that the maximum distortion, as well as the minimum crystallite size, correspond to x = 0.

Fig. 2: shows the Fourier transform infrared absorption (FTIR) spectra for the investigated samples. The spectra show 3 absorption bands in the short wavelengths, while in the long wavelength the absorption peaks cease to exist up to 4000 cm^{-1}. The vibrational absorption peaks are attributed to the stretching and bending modes of the oxygen cation complexes. The observed peaks follow the factor group prediction for perovskite structure [27–30]. The absorption band at 430 nm seems to be sensitive to the cell distortion factor, which decreases as the metal concentration x increase, shown in Fig. 1c. It can be observed that the most of the bands are shifted to the lower wavenumbers with increasing the dopant (except x = 0.2 for ν_s), that is due to the expected difference in the ionic radius where the ionic radius of La^{+3} and Fe^{+3} is larger than the ionic radius of Ca^{+2} and Ti^{+4}. It is also noticed that all ν_b bands are shifted to lower wavenumbers, which suggest an increase in the angle O-Fe/Ti-O as the substituted cations concentration increases.

Fig. 3: Shows the magnetic hysteresis loop for the perovskite structure, it can be seen that for the sample of x = 0.2, 0.3 have similar magnetization behavior, while the saturation magnetization

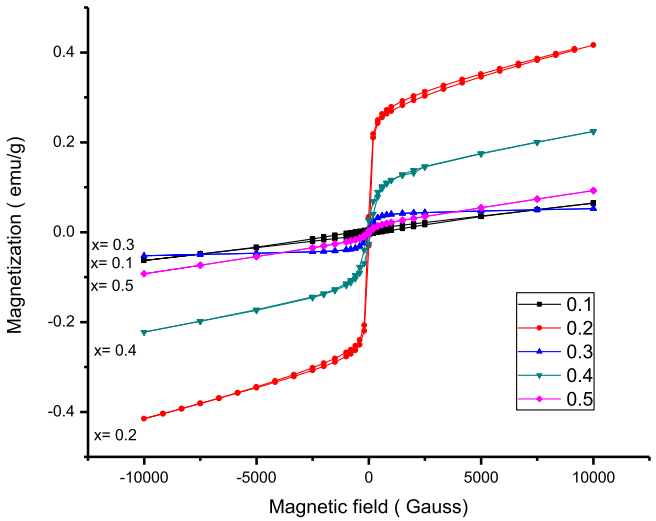

Fig. 3. Magnetic hysteresis loops of $Ca_{1-x}La_xTi_{1-x}Fe_xO_3$.

decreases for the rest of samples as x increases for x = 0.1, 0.4, and 0.5.We should note that 0.5 is the less distorted sample. Hence we expect x = 0.5 to exhibit the lowest electrical polarization. The decrease in the saturation magnetization is due to the antiferromagnetic structure. The exchange interaction in return is decreased. However at x = 0.2 the saturation magnetization shows its maximum value, while it shows its lowest values for x = 0.1 and 0.5. That could be due to the strong hybridization of the outermost orbitals in the crystal lattice which induces the electrical polarization.

Fig. 4: Depicts the variation of the saturation magnetization and the remnant magnetization with increasing temperature, both parameters show a slight decrease with temperature increase. The saturation magnetization shows a dip at T = 150 K. The magnetization parameters and the canting angle are shown in table 1. It can be seen that the canting angle (Ti/Fe-O_1-Ti/Fe) decreases with increasing x. The decrease in the saturation magnetization with increasing x is then due to increasing both the La–O and Fe–O distances .The origin of enhanced M at x = 0.2 might be caused by the distorted spiral magnetic order. The superexchange interaction increases slightly then drop at x = 0.4 then increases again, the behavior is similar to the electrical polarization behavior of the same sample, that concludes that the electrical polarization in that sample is magnetic based. In other words, the crystal distortion

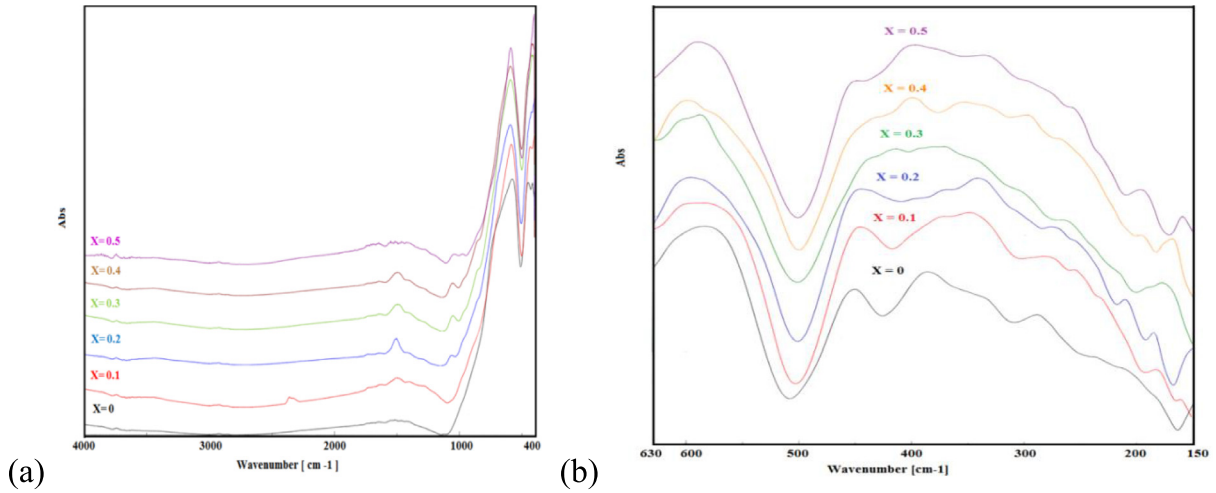

Fig. 2. (a and b): IR absorption spectra for $Ca_{1-x}La_xTi_{1-x}Fe_xO_3$ at the ranges 400–4000 cm^{-1} and 150–630 cm^{-1} respectively.

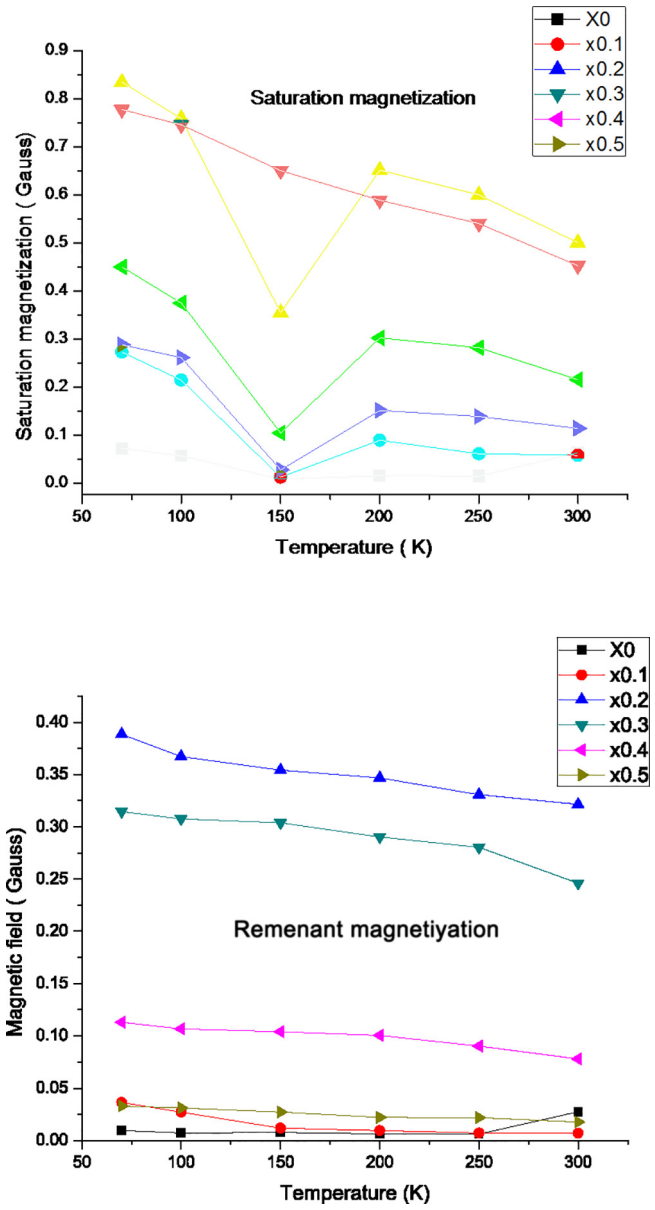

Fig. 4. Saturation, and remenant magnetization Ms, Mr. as a function of x at different temperature.

due to doping is affecting the superexchange interaction based on the canting angle, and the strength of the d-shell hybridization. Hence, the magnetically driven ferro-electricity is one reason for the polarization behavior in that type of perovskite (Table 2).

Fig. 5 Shows the variation of the electric hysteresis with varying the doping parameter x. only a slight change in the remnant polarization can be noticed. The data reveals a slight change in the polarization data as well as the remnant polarization. The similarity of the electrical and magnetic polarization behavior suggests

Table 2
Electric hysteresis parameters of Ca1-xLaxTi1-xFexO3, 0.1⩽x⩽0.5.

Concentration	P_m	P_r	E_c
0.0	42.5	23	273
0.2	41	28	257
0.3	42	25	206
0.4	55	32	278
0.5	34	18	227

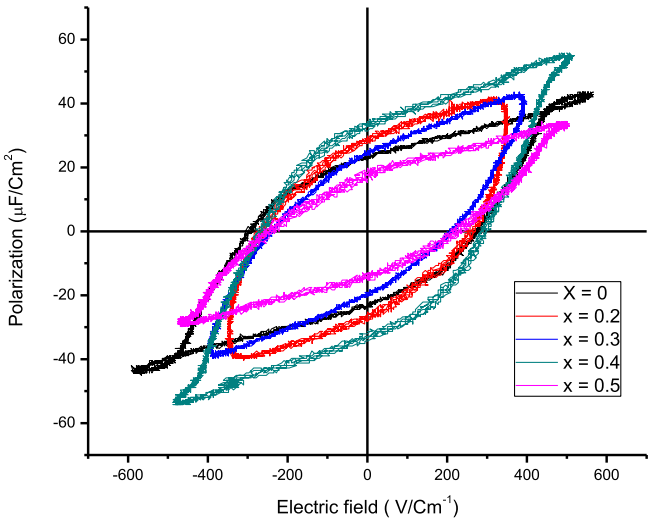

Fig. 5. Shows P-E curves of $Ca_{1-x}La_xTi_{1-x}Fe_xO_3$for x = 0, 0.2, 0.3, 0.4 and 0.5.

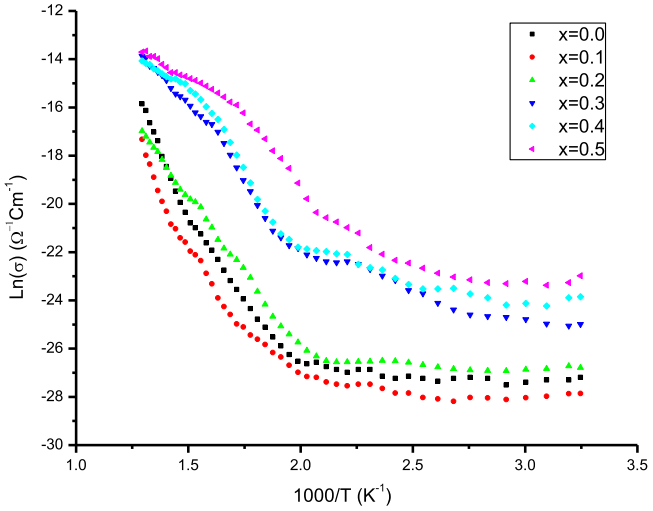

Fig. 6. Arrhenius plot of the conductivity for different La^{3+} ion doped Ca-Titanate perovskite structure.

that the ferroelectricity of the samples is magnetic driven. A crucial parameter is an electrical conductivity is shown in Fig. 6. The vari-

Table 1
Magnetic parameters of Ca1-xLaxTi1-xFexO3, 0.1⩽x⩽0.5.

Super-exchange angle (Ti/Fe-O_2-Ti/Fe) (°)	Canting angle (Ti/Fe-O_1-Ti/Fe) (°)	Squareness	H_c(G)	M_r (emu/g)	M_s (emu/g)	x
157.30 (4)	159.01 (1)	0.080	583.34	5.077E−3	63.85 E−3	0.1
159.57 (6)	157.29 (2)	0.076	26.500	31.88E−3	417.07 E−3	0.2
165.51 (8)	157.05 (2)	0.123	48.48	25.00E−3	374 E−3	0.3
158.08 (8)	154.5 (3)	0.119	79.70	26.5E−3	223.4 E−3	0.4
166.38 (12)	146.35 (3)	0.034	64.93	3.157E−3	92.62 E−3	0.5

ation of ln(σ) with 1000/T, known as the Arrhenius plot, shows that the conductivity follows the same trend as the electrical polarization. The perovskite samples are consists of grains and grain boundaries. The grain boundaries are more sensitive to AC- electric field which results in a circumferential current around the grain. The circumferential current results in an internal magnetic field that takes part in the magnetic ordering.

4. Conclusion

We reported for the first time the correlation of the magnetic and ferroelectric properties in the compound $CaTiO_3$ doped La, Fe. The compound has a perovskite structure of a noncentrosymmetric space group Pbnm. The symmetry group allows the ferroelectricity as a function of crystal distortion. We have shown that inducing the multiferroic property can be done by multiple element doping. The multiple dopant cause symmetry breaks which induce both electric and magnetic ordering. The maximum distortion was found for x = 0, which corresponds to $CaTiO_3$. The experimental results of the magnetization and electrical polarization are consistent with the previously published work on structural Rietveld analysis. The maximum distortion corresponds to the maximum correlation of the ferromagnetic and ferroelectric property of the compound at the same x value. As the x value increases the crystal structure approaches pseudo-tetragonal perovskite structure with minimum crystal distortion at x = 0.5. Hence the electrical polarization is reduced and the coupling between magnetic and electric order gets weaker.

References

[1] V.R. Palkar, D.C. Kundaliya, S.K. Malik, S. Bhattacharya, Magnetoelectricity at room temperature in the $Bi_{0.9}-xTbxLa_{0.1}FeO_3$ system, Phys. Rev. B 69 (21) (Jun. 2004) 212102.

[2] J. Zhai, N. Cai, Z. Shi, Y. Lin, C.-W. Nan, Magnetic-dielectric properties of $NiFe_{2O}4$/PZT particulate composites, J. Phys. D Appl. Phys. 37 (6) (Mar. 2004) 823–827.

[3] M.P. Singh, W. Prellier, L. Mechin, C. Simon, B. Raveau, Correlation between structure and properties in multiferroic La0.7Ca0.3MnO3/BaTiO3 superlattices, J. Appl. Phys. 99 (2) (Jan. 2006) 24105.

[4] Multiferroic and piezoelectric properties of 0.65BiFeO3–0.35BaTiO3 ceramic with pseudo-cubic symmetry, Ceram. Int., 38(4) (2012) 3499–3502.

[5] Influence of doping concentration on room-temperature ferromagnetism for Fe-doped BaTiO3 ceramics, J. Magn. Magn. Mater., 320(5) (2008) 691–694.

[6] H. Schmid, Some symmetry aspects of ferroics and single phase multiferroics*, J. Phys. Condens. Matter 20 (43) (Oct. 2008) 434201.

[7] M.H. Abdellatif, C. Innocenti, I. Liakos, A. Scarpellini, S. Marras, M. Salerno, Effect of Jahn-Teller distortion on the short range magnetic order in copper ferrite, J. Magn. Magn. Mater. (2017).

[8] M.H. Abdellatif, J.D. Song, W.J. Choi, N.K. Cho, In/Ga inter-diffusion in InAs quantum dot in InGaAs/GaAs asymmetric quantum well, J. Nanosci. Nanotechnol. 12 (7) (Jul. 2012) 5774–5777.

[9] J. Wang et al., Epitaxial BiFeO3 multiferroic thin film heterostructures, Science 299 (5613) (Mar. 2003) 1719–1722.

[10] T. Kimura, T. Goto, H. Shintani, K. Ishizaka, T. Arima, Y. Tokura, Magnetic control of ferroelectric polarization, Nature 426 (6962) (Nov. 2003) 55–58.

[11] N. Hur, S. Park, P.A. Sharma, J.S. Ahn, S. Guha, S.-W. Cheong, Electric polarization reversal and memory in a multiferroic material induced by magnetic fields, Nature 429 (6990) (May 2004) 392–395.

[12] D. Khomskii, Classifying multiferroics: mechanisms and effects, Physics (College. Park. Md) 2 (2009) 20.

[13] D.I. Khomskii, Multiferroics: different ways to combine magnetism and ferroelectricity, J. Magn. Magn. Mater. 306 (1) (Nov. 2006) 1–8.

[14] M. Fiebig, Revival of the magnetoelectric effect, J. Phys. D Appl. Phys. 38 (8) (Apr. 2005) R123–R152.

[15] A.M. Kadomtseva, A.K. Zvezdin, Y.F. Popov, A.P. Pyatakov, G.P. Vorob'ev, Space-time parity violation and magnetoelectric interactions in antiferromagnets, J. Exp. Theor. Phys. Lett. 79 (11) (2004) 571–581.

[16] M.H. Abdellatif, G.M. El-Komy, A.A. Azab, Magnetic characterization of rare earth doped spinel ferrite, J. Magn. Magn. Mater. (2017).

[17] M.H. Abdellatif, G.M. El-Komy, A.A. Azab, A.M. Moustafa, Oscillator strength and dispersive energy of dipoles in ferrite thin film, Mater. Res. Express 4 (7) (Jul. 2017) 76410.

[18] Crystal field distortion of La3+ ion-doped Mn-Cr ferrite, J. Magn. Magn. Mater., 447 (2018) 15–20.

[19] M.H. Abdellatif, A.A. Azab, M. Salerno, Effect of rare earth doping on the vibrational spectra of spinel Mn-Cr ferrite, Mater. Res. Bull. 97 (2018) 260–264.

[20] E. Ascher, H. Rieder, H. Schmid, H. Stössel, Some properties of ferromagnetoelectric nickel-iodine boracite, $Ni_3B_7O_{13}I$, J. Appl. Phys. 37 (3) (Mar. 1966) 1404–1405.

[21] R. Börnstein, K.-H. Hellwege, H. Landolt, O. Madelung, T. Mitsui, Landolt-Börnstein Zahlenwerte und Funktionen aus Naturwissenschaften und Technik: Neue Serie = Numerical data and functional relationships in science and technology: new series Gruppe 3 Kristall- und Festkörperphysik = Crystal and solid state physics Bd. 16 Ferroelektrika und verwandte Substanzen : Neubearbeitung und Erweiterung der Bände 3/3 und 3/9 = Ferroelectrics and related substances Teilbd. a Oxide, Springer, 1981.

[22] M.H. Abdellatif, A.A. Azab, A.M. Moustafa, Dielectric spectroscopy of localized electrical charges in ferrite thin film, J. Electron. Mater. (2017) 1–7.

[23] M.A. Abdellatif Mohamed, Ferrites, Theory and Applications, LAP LAMPERT Academic Publishing, 2017, 978-3-330-07427-9, 3330074272,9783330074279.

[24] L. Moustafa, I.S. Ahmed Farag, L.M. Salah, Structural characterization of substituted calcium titanate compounds Ca1-XLaXTi1-xFexO3, Egypt. J. Solids 27 (2004) 213–222.

[25] M. Stewart, M. Cain, D. Hall, Ferroelectric hysteresis measurement and analysis, 1999.

[26] S.H. Morgan, E. Silberman, J.M. Springer, Laboratory experiment on the measurement of pyroelectric coefficients, Am. J. Phys. 52 (6) (Jun. 1984) 542–545.

[27] K. Kaswan, A. Agarwal, S. Sanghi, M. Rangi, S. Jangra, A. Kumar, Crystal structure refinement, enhanced magnetic and dielectric properties of Na0.5Bi0.5TiO3 modified Bi0.8Ba0.2FeO3 ceramics, Ceram. Int. 43 (5) (2017) 4622–4629.

[28] M.A. Islam, J.M. Rondinelli, J.E. Spanier, Normal Mode Determination of Perovskite Crystal Structures with Octahedral Rotations: Theory and Applications, 2013.

[29] B.A. Dpaxcul, R.E. Npwnnlm, A. Wrr, Factor group analysis of the vibrational spectra of crystals: a review and consolidation, Am. Mineral. 57 (1972) 255–268.

[30] Q. Williams, R. Jeanloz, P. McMillan, Vibrational spectrum of $MgSiO_3$ perovskite: zero-pressure Raman and mid-infrared spectra to 27 GPa, J. Geophys. Res. 92 (B8) (Jul. 1987) 8116.